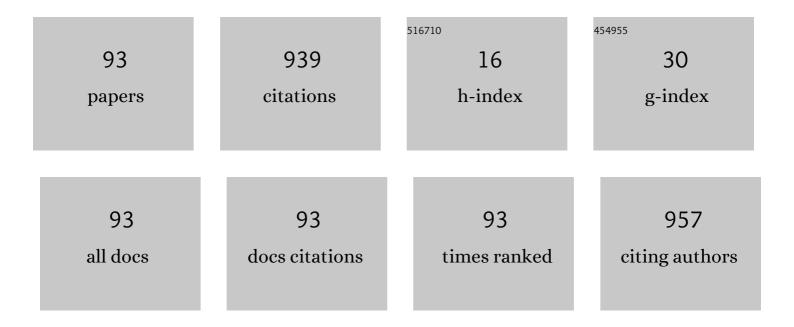
List of Publications by Year in descending order

Source: https://exaly.com/author-pdf/2367843/publications.pdf Version: 2024-02-01



IEAN-FU KIANC

#	Article	IF	CITATIONS
1	Dual-Band Circularly Polarized Cavity-Backed Annular Slot Antenna for GPS Receiver. IEEE Transactions on Antennas and Propagation, 2012, 60, 2076-2080.	5.1	114
2	Compact Multi-Band H-Shaped Slot Antenna. IEEE Transactions on Antennas and Propagation, 2013, 61, 4345-4349.	5.1	85
3	Design of Wideband LNAs Using Parallel-to-Series Resonant Matching Network Between Common-Gate and Common-Source Stages. IEEE Transactions on Microwave Theory and Techniques, 2011, 59, 2285-2294.	4.6	72
4	Comparison of CNN Algorithms on Hyperspectral Image Classification in Agricultural Lands. Sensors, 2020, 20, 1734.	3.8	58
5	Dualband Split Dielectric Resonator Antenna. IEEE Transactions on Antennas and Propagation, 2007, 55, 3155-3162.	5.1	48
6	A 30 GHz Active Quasi-Circulator With Current-Reuse Technique in <formula formulatype="inline"> <tex notation="TeX">\$0.18~mu{m m}\$</tex> CMOS Technology. IEEE Microwave and Wireless Components Letters, 2010, 20, 693-695.</formula 	3.2	47
7	Optimization of Sparse Linear Arrays Using Harmony Search Algorithms. IEEE Transactions on Antennas and Propagation, 2015, 63, 4732-4738.	5.1	47
8	A 5-GHz CMOS Frequency Synthesizer With an Injection-Locked Frequency Divider and Differential Switched Capacitors. IEEE Transactions on Circuits and Systems I: Regular Papers, 2009, 56, 320-326.	5.4	42
9	Effect of Mutual Coupling on the Channel Capacity of MIMO Systems. IEEE Transactions on Vehicular Technology, 2016, 65, 398-403.	6.3	37
10	Bandwidth Broadening of Dielectric Resonator Antenna by Merging Adjacent Bands. IEEE Transactions on Antennas and Propagation, 2009, 57, 3316-3320.	5.1	33
11	Modeling of ionospheric perturbation by 2004 Sumatra tsunami. Radio Science, 2009, 44, .	1.6	32
12	Wideband Dielectric Resonator Antenna With a Tunnel. IEEE Antennas and Wireless Propagation Letters, 2008, 7, 275-278.	4.0	28
13	A Domain Decomposition Finite Difference Time Domain (FDTD) Method for Scattering Problem from Very Large Rough Surfaces. IEEE Transactions on Antennas and Propagation, 2015, 63, 4468-4476.	5.1	25
14	Estimation on Location, Velocity, and Acceleration With High Precision for Collision Avoidance. IEEE Transactions on Intelligent Transportation Systems, 2010, 11, 374-379.	8.0	24
15	Broadband Dielectric Resonator Antenna With an Offset Well. IEEE Antennas and Wireless Propagation Letters, 2007, 6, 564-567.	4.0	23
16	A 0.18 \$mu{m m}\$ CMOS Self-Mixing Frequency Tripler. IEEE Microwave and Wireless Components Letters, 2012, 22, 79-81.	3.2	19
17	OOK/BPSK-Modulated Impulse Transmitters Integrated With Leakage-Cancelling Circuit. IEEE Transactions on Microwave Theory and Techniques, 2013, 61, 218-224.	4.6	15
18	Comparison of Injection-Locked and Coupled Oscillator Arrays for Beamforming. IEEE Transactions on Microwave Theory and Techniques, 2015, 63, 1353-1360.	4.6	15

#	Article	IF	CITATIONS
19	Attenuation of Millimeter-Wave in a Sand and Dust Storm. IEEE Geoscience and Remote Sensing Letters, 2016, 13, 1094-1098.	3.1	13
20	Sectorial-Beam Dielectric Resonator Antenna for WiMAX With Bent Ground Plane. IEEE Transactions on Antennas and Propagation, 2009, 57, 563-567.	5.1	12
21	Adjustment of Beamwidth and Side-Lobe Level of Large Phased-Arrays Using Particle Swarm Optimization Technique. IEEE Transactions on Antennas and Propagation, 2014, 62, 138-144.	5.1	11
22	DUCTING AND TURBULENCE EFFECTS ON RADIO-WAVE PROPAGATION IN AN ATMOSPHERIC BOUNDARY LAYER. Progress in Electromagnetics Research B, 2014, 60, 301-315.	1.0	10
23	Optimization of Asymmetrical Difference Pattern With Memetic Algorithm. IEEE Transactions on Antennas and Propagation, 2014, 62, 2297-2302.	5.1	10
24	PWE-Based Radar Equation to Predict Backscattering of Millimeter-Wave in a Sand and Dust Storm. IEEE Transactions on Antennas and Propagation, 2017, 65, 785-793.	5.1	9
25	RFID Regulator Design Insensitive to Supply Voltage Ripple and Temperature Variation. IEEE Transactions on Circuits and Systems II: Express Briefs, 2010, 57, 255-259.	3.0	8
26	Small Broadband Antenna Composed of Dual-Meander Folded Loop and Disk-Loaded Monopole. IEEE Transactions on Antennas and Propagation, 2011, 59, 1716-1720.	5.1	8
27	Simulation of X-Band Signals in a Sand and Dust Storm With Parabolic Wave Equation Method and Two-Ray Model. IEEE Antennas and Wireless Propagation Letters, 2017, 16, 238-241.	4.0	8
28	Joint Estimation of DOA and Frequency of Multiple Sources with Orthogonal Coprime Arrays. Sensors, 2019, 19, 335.	3.8	7
29	Analysis of a CPW-fed slot ring antenna. , 0, , .		6
30	Coupling Characterization of a Linear Dipole Array to Improve Direction-of-Arrival Estimation. IEEE Transactions on Antennas and Propagation, 2015, 63, 5056-5062.	5.1	6
31	Characteristics of striplines with inhomogeneous cylindrical substrate. IEEE Transactions on Microwave Theory and Techniques, 2003, 51, 1496-1505.	4.6	5
32	Quadrifilar helix antenna for GPS applications. , 0, , .		5
33	Multipath effects on beacon performances. , 0, , .		4
34	Charge Recycling Method on Pixel Level. Journal of Display Technology, 2008, 4, 211-217.	1.2	4
35	A direct-conversion UWB RF front-end for MB-OFDM application. , 2009, , .		4
36	A Small Broadband Folded-Loop Antenna With Disk-Loaded Monopole. IEEE Antennas and Wireless Propagation Letters, 2010, 9, 1248-1250.	4.0	4

#	Article	IF	CITATIONS
37	AN IMPROVED RANGE-DOPPLER ALGORITHM FOR SAR IMAGING AT HIGH SQUINT ANGLES. Progress in Electromagnetics Research M, 2017, 53, 41-52.	0.9	4
38	Improved chirp scaling algorithms for SAR imaging under high squint angles. IET Radar, Sonar and Navigation, 2017, 11, 1629-1636.	1.8	4
39	Long-range pulse propagation over different surfaces using domain-decomposition FDTD method. , 2011, , .		3
40	Efficient carrier frequency offset estimation for orthogonal frequencyâ€division multiple access uplink with an arbitrary number of subscriber stations. IET Communications, 2014, 8, 199-209.	2.2	3
41	Dispersion properties of circular dielectric waveguides loaded with periodic metal disks. Microwave and Optical Technology Letters, 2007, 49, 2057-2061.	1.4	2
42	CMOS-MEMS single-axis magnetic-field sensor for measuring geomagnetic field disturbance. , 2010, , .		2
43	A ray tracing technique for radio occultation. , 2011, , .		2
44	Chirp scaling algorithms for SAR imaging under high squint angles. , 2017, , .		2
45	SAR IMAGING ON HEO SATELLITES WITH AN IMPROVED FREQUENCY-DOMAIN ALGORITHM. Progress in Electromagnetics Research M, 2017, 55, 189-201.	0.9	2
46	Brightness Temperatures From Very Lossy Medium With Near-Field Bistatic Transmission Coefficients. IEEE Transactions on Geoscience and Remote Sensing, 2019, 57, 4407-4416.	6.3	2
47	Dispersive FDTD Scheme and Surface Impedance Boundary Condition for Modeling Pulse Propagation in Very Lossy Medium. IEEE Transactions on Antennas and Propagation, 2020, 68, 3060-3067.	5.1	2
48	Estimation of rangeâ€dependent soundâ€speed profile with dictionary learning method. IET Radar, Sonar and Navigation, 2020, 14, 194-199.	1.8	2
49	Dispersion analysis of microstrip lines with nonrectangular cross-sections. , 0, , .		1
50	Characteristics of striplines with inhomogeneous cylindrical substrate. , 0, , .		1
51	Dual-band dielectric resonant antenna. , 2004, , .		1
52	Design Constraints on FSC LCD. IEEE Transactions on Electron Devices, 2008, 55, 533-539.	3.0	1
53	Active and Adaptive Charging Method on Data Lines for Delay Compensation. Journal of Display Technology, 2008, 4, 198-203.	1.2	1
54	Three-axis accelerometer in CMOS MEMS. , 2009, , .		1

4

0

#	Article	IF	CITATIONS
55	Reconstruction algorithm applied to low-frequency array (LOFAR) image. , 2011, , .		1
56	Beam steering of a large phased-array antenna with fixed major-lobe beamwidth and side-lobe levels. , 2013, , .		1
57	Electroquasistatic model of RF capacitive hyperthermia with heat convection mechanism. , 2017, , .		1
58	Water-Table Detection in a Hyper-Arid Region. , 2019, , .		1
59	Comparative Study on Planetary Magnetosphere in the Solar System. Sensors, 2020, 20, 1673.	3.8	1
60	Frequency-selective behavior of layered dielectric periodical structures for TE case. , 0, , .		0
61	Analysis of coplanar waveguide-fed circular patch antenna. , 0, , .		0
62	Scattering analysis of strip gratings with layered periodical substrate for TE case. , 0, , .		0
63	Dispersion characteristics of the anisotropic dielectric strip waveguides with trapezoidal cross-section. , 0, , .		0
64	Partially loaded periodic microstrip lines. , 0, , .		0
65	Mesh antennas with reduced size. , 2004, , .		0
66	Bandwidth enhancement by merging resonant modes of dielectric resonator antenna. , 2007, , .		0
67	Modeling of tsinami-induced ionospheric irregularities. , 2008, , .		0
68	Design of FMCW radar transceiver at 24 GHz. Digest / IEEE Antennas and Propagation Society International Symposium, 2009, , .	0.0	0
69	Free-floating GPS sensor network for tsunami detection. , 2009, , .		0
70	A CMOS-MEMS single-chip dual-axis gyroscope. , 2009, , .		0
71	Fractional-N frequency synthesizer at 24 GHz. , 2010, , .		0

A small wideband folded meander loop antenna with three coupled modes. , 2010, , .

5

#	Article	IF	CITATIONS
73	Electromagnetic signatures of earthquake preparation. , 2010, , .		Ο
74	Dropsondes with DGPS for real-time typhoon monitoring. , 2010, , .		0
75	Design of dual-axis accelerometer with CMOS-MEMS. , 2010, , .		0
76	A 4-bit MEMS phase shifter at 24 GHz based on lateral MEMS switches. , 2010, , .		0
77	Implementation of accelerometer in CMOS-MEMS. , 2010, , .		0
78	Stereoâ€synthetic aperture radar technique with bias correction to estimate terrain height. IET Radar, Sonar and Navigation, 2013, 7, 225-232.	1.8	0
79	A Domain Decomposition Finite Difference Time Domain (DD-FDTD) method for solving the scattering problem from very large rough surfaces. , 2014, , .		Ο
80	Highly accurate direction-of-arrival estimation with a uniform circular array. , 2014, , .		0
81	A multi-feature visibility processing algorithm for radio interferometric imaging. , 2014, , .		0
82	A multi-feature visibility processing algorithm for radio interferometric imaging. , 2015, , .		0
83	An Iterative Approach to Improve Images of Multiple Targets and Targets with Layered or Continuous Profile. International Journal of Microwave Science and Technology, 2015, 2015, 1-13.	0.6	0
84	A domain decomposition FDTD method for scattering from very large rough surfaces. , 2015, , .		0
85	Retrieval of major greenhouse gas profiles with LEO-ground infrared laser occultation (LGIO) technique. , 2015, , .		Ο
86	Improved millimeter-wave radar equations to predict backscattering in a sand-and-dust storm. , 2017, , .		0
87	Synthetic Aperture Radar Imaging on Lunar Surface with Observatory on Earth. , 2018, , .		0
88	Efficacy of Magnetic and Capacitive Hyperthermia on Hepatocellular Carcinoma. , 2018, , .		0
89	Brightness Temperature from Very Lossy Medium. , 2018, , .		0
90	Brightness Temperatures From Layered Lossy Medium With Rough Surfaces by Combining FDTD and Coherent Methods. IEEE Geoscience and Remote Sensing Letters, 2019, 16, 1085-1089.	3.1	0

#	Article	IF	CITATIONS
91	Comparison of Algorithms and Input Vectors for Sea-Ice Classification with L-band PolSAR Data. , 2019, , .		0
92	Simulations of Switchback, Fragmentation and Sunspot Pair in δ-Sunspots during Magnetic Flux Emergence. Sensors, 2021, 21, 586.	3.8	0
93	Analysis of an MIS transmission line with a depletion region. , 0, , .		0